Exercises and Study Guide

The Physics and Chemistry of the Interstellar Medium

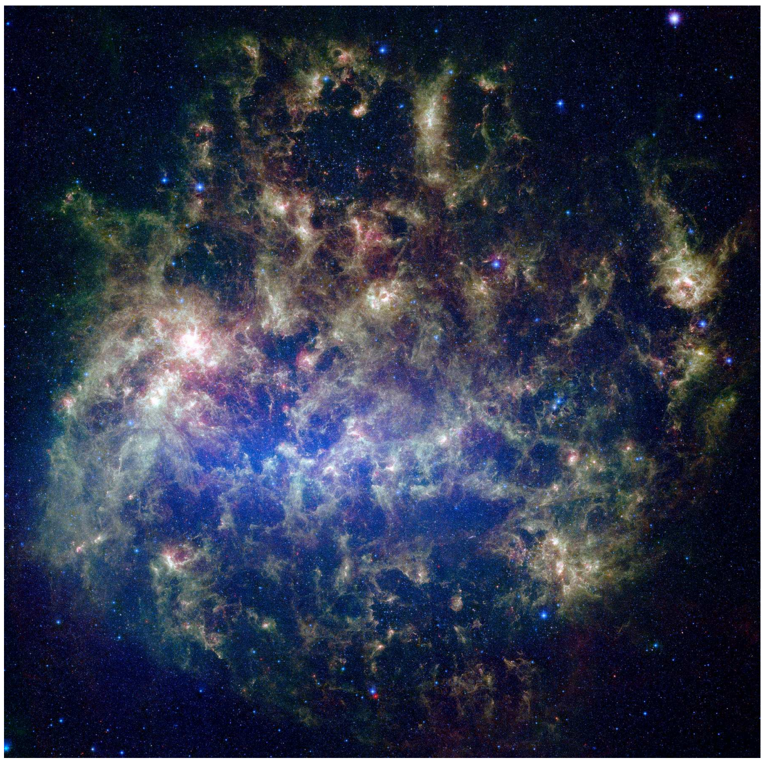

A.G.G.M. Tielens

September 2006

Preface

This set of exercises and study guide has been developed for use with the text book "The Physics and Chemistry of the Interstellar Medium" (A.G.G.M. Tielens, 2005, Cambridge University Press: ISBN-13 978-0-521-82634-9). Note that errata for the first printing are provided on the Cambridge University website: http://www.cambridge.org/catalogue/catalogue.asp?isbn=0521826349 under the button for online support material and you should get those before embarking on these exercises.

The set of exercises were developed over several years teaching this course and they serve several aims. First, I like to discuss many of the simple estimates included here during the actual lectures to provide the students with a back-off-the-envelope feeling for the problem. Second, some exercises are meant to force the student to derive relationships given in the text. For many students, deriving an equation gives them a better grip on the issues involved, as well as forces them to assimilate the text. Third, some exercises are included for the students to work out 'real' problems such as deriving physical conditions from observations. This provides the student with valable hands-on experience in working with these difficult matters. Finally, I have also included some questions which should help the student focus on what they are supposed to have learned in a chapter. These 'compare and contrast' questions are not meant to lead to long essays but rather to a short synopsis of the key processes or issues. To the instructor, these questions provide a good way of stimulating participation in a class setting and to gauche how well the students have absorbed the subject.

To the students: Do not feel discouraged if you are unable to immediately solve these exercises. It took me five years to write this book and develop these questions and it took me a lifetime to get the hang of the interstellar medium. In my experience, persistency always pays off and your time will come.

Acknowledgements I am very grateful to Jacquie Keane, Leticia Martín-Hernández, Chris Ormel, and Els Peeters for assistance in developing these exercises.

1.1 Chapter 1

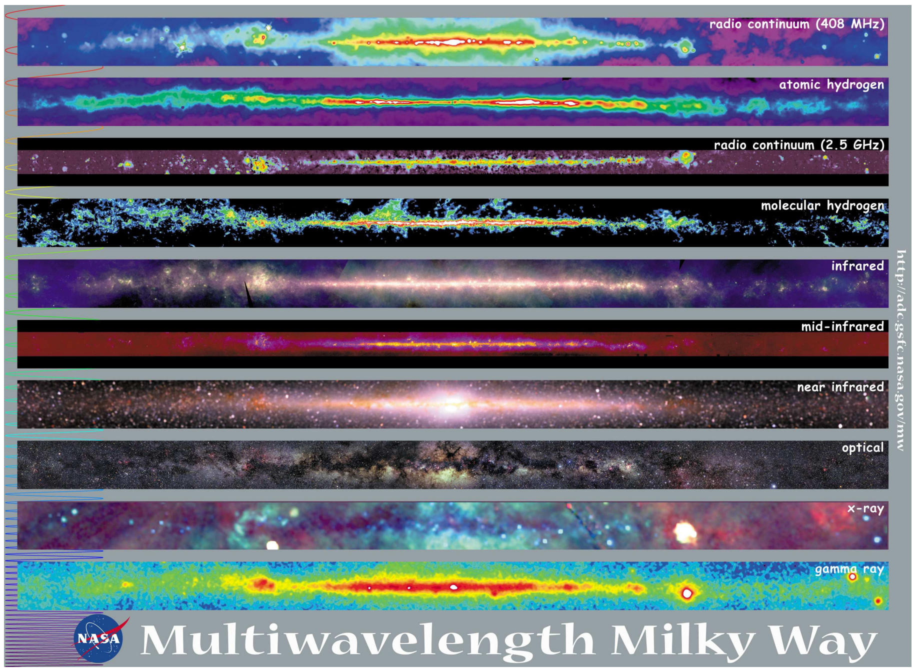

Figure 1.1: *The multiwavelength interstellar medium: maps of the Milky Way at ten wavelengths, from radio waves to gamma rays. Taken from the website: http://adc.gsfc.nasa.gov/mw/milkyway.html*

1. The multiwavelength Milky Way

   Figure 1.1 shows a set of images of the Milky Way at wavelengths ranging from γ-rays to the radio regime. These are taken from the website, http://adc.gsfc.nasa.gov/mw/milkyway.html, and you should go to this url for this exercise. This data allows for a quick comparison of the Milky Way at these different wavelength. Perusal of these images can be very illuminating. The aim of this exercise is to gain an understanding of what objects show up at certain wavelengths.

   (a) Give two reasons why the galactic plane is hardly visible at optical wavelengths while it is very prominent at near-infrared through far-infrared wavelengths.

   (b) Explain why the mid-plane of the galaxy is dominated by relatively hard X-ray emission (1.5 keV), while emission at 0.25 keV dominates at higher lattitudes.

(c) Why is the diffuse γ-ray emission an excellent tracer of interstellar gas ?

(d) Describe and explain the appearance of the supernova remnant, Cas A ($\ell = 112^{\rm o}$), at the various wavelengths.

(e) At $(\ell, b) = (50, 0)^{\rm o}$, a discrete object is visible at certain wavelengths. What kind of object might this be ? Explain your answer.

(f) Explain why the Crab pulsar is visible (at $\ell = 185^{\rm o}$) in the radio, X-ray, and γ-ray maps.

2. Many molecules are ionized or dissociated by photons in the range 6-13.6 eV. For the interstellar radiation field (eqn (1.1)), calculate the mean photon intensity in this range. Some species (eg., H_2, CO, and C) are only affected by photons above 11 eV. Calculate the mean photon intensity in this range as well.

3. Contrast and compare the emission spectra of HII regions, reflection nebula, dark nebula, photodissociation regions, and supernova remnants and link these differences to the relevant physical processes.

4. Contrast and compare the emission spectra of the Warm Neutral Medium, the Warm Ionized Medium, and the Hot Intercloud Medium.

5. Based upon their spectral characteristics, try to link the different phases of the interstellar medium to classes of objects. What does this suggest about the physical processes involved in the phase structure of the ISM ?

6. The vertical distribution of the various phases of the ISM are very different (cf., Table 1.1). What could be the cause ?

7. Compare and contrast the characteristics of interstellar dust and interstellar PAHs.

8. Examine the different energy sources for diffuse clouds in table 1.2 and section 1.3. Many of these have very similar energy densities. Why, then, do the heating rates differ by over an order of magnitude ?

9. Take on a lotus position and contemplate thermodynamic equilibrium. In order to become one with the universe, equilibrium is preferred. However, astronomers like the opposite. Why would that be ?

1.2 Chapter 2

1. Calculate the force constants from the vibrational frequency of the stretching vibration in CO ($\nu = 2140$ cm^{-1}). In what sense would the force constant change for the CO transition in a carbonyl and in an ether ?

2. Rotational spectroscopy: Consider CO as a linear, rigid rotor.

(a) The frequency of the J=1-0 transition of the main isotope of CO ($^{12}C^{16}O$) is 115.3 GHz. What is the internuclear distance in this molecule ?

(b) How large a frequency shift can be expected for the J=1-0 transition in the $^{13}C^{16}O$ isotope ? (Hint: the internuclear distance will not change).

3. Derive the approximation for the partition function on the right-hand-side of equation (2.14) (Hint: approximate the summation by an integration).

4. Calculate the Einstein A transition probability for the $J = 1-0$ transition of CO. The dipole moment of CO is 0.108 Debey.

5. The line averaged optical depth, corrected for stimulated emission is given by,

$$\tau_{ul} \;=\; (n_l B_{lu} \;-\; n_u B_{ul})\; h\nu_{ul}\, \frac{\Delta z}{\Delta \nu} \tag{1.1}$$

with $\Delta\nu$ the linewidth. Using the relationships between the Einstein coefficients (Eq. (2.16-2.18), derive expression Eq. (2.43).

6. Derive an heuristic expression for the escape probability by considering the decrease in the intensity emitted at optical depth τ and averaging this over the slab (eg., calculate $\langle \exp\left[-\tau\right] \rangle$). What is the physical significance of the $1/\tau$ dependence for large τ ? More exact approaches average this escape factor over direction and/or frequency, but the significance is the same.

7. Derive the expression for the emergent intensity from a homogeneous, plane parallel, semi-infinite slab (Eq. (2.47) and (2.48) from equation (2.46) using equations (2.20) (neglecting background radiation), (2.43), and (2.44). Check both limits (eqn. (2.49) and (2.50)).

8. CO rotational emission:

(a) Assuming optically thin emission in LTE, what is the expected intensity of the $J = 1-0$ line for a column of 10^{15} CO molecules cm^{-2} at $T = 10$ K ?

(b) For a line width of 2 km/s, what is the corresponding peak brightness temperature ?

(c) What is the expected optically thick peak brightness temperature for the line ?

(d) The measured peak brightness temperatures for the two main isotopes of CO are $T_B\left(^{12}C^{16}O\right) = 12.4$ K and $T_B\left(^{12}C^{16}O\right) = 4.9$ K. Assuming that $^{12}C^{16}O$ is optically thick and $^{13}C^{16}O$ is optically thin and adopting a $^{12}C^{16}O/^{13}C^{16}O$ ratio of 65, what is the column density of $^{12}C^{16}O$?

9. CO rovibrational absorption. Consider a strong mid-infrared source (intensity I_0) behind a cold ($T = 10$ K) foreground molecular cloud with a CO column density of 10^{17} cm^{-2}.

   (a) Starting from Eq. (2.2) for a harmonic oscillator and a rigid rotor, derive the ro-vibrational absorption pattern of CO molecules in the spectrum of the background source.

   (b) The Einstein A coefficient for the transition from $(v = 1, J'') \rightarrow to (v = 0, J')$ is given by

   $$A_{ul} = \frac{64\pi^4\tilde{\nu}^3}{3h} |\mu_v|^2 \frac{L(J'')}{g_u} \quad , \tag{1.2}$$

   with $\tilde{\nu}$ the frequency of the transition in cm^{-1}, μ_v is the dipole moment (0.108 D for CO), and $L(J'')$ the Hönl-London factor which for a linear molecule is given by J'' for the P-branch and $J'' + 1$ for the R-branch. Assuming thermodynamic equilibrium, calculate the population of a number of low-lying lines, and the optical depth in the relevant transitions, and sketch the spectrum.

   (c) In what sense would the spectrum change if the temperature were 100 K ?

10. The cooling of the phases of the ISM

    (a) Adopting the characteristics of the different phases in Table 1.1, estimate the cooling rate per atom in the HIM, WNM, and CNM from Figure 2.10.

    (b) Adopting the total masses of gas in these different phases given in Table 1.1, show that the total luminosities are $\sim 10^{40}$, $\sim 5 \times 10^{40}$, and $\sim 3 \times 10^{41}$ erg s^{-1} for the HIM, WNM, and CNM, respectively.

    (c) Explain why – while the total luminosity of the CNM is substantially larger than the luminosity of the other phases – the other phases can still be readily observed.

11. List the Bracket lines (Hα, Hβ, Hγ, ...) in order of increasing Einstein A transition coefficient. Do the same for the Lyman α, Bracket α, and Paschen α transitions. Explain your ordering.

12. The optical spectra of laboratory plasma's are characterized by allowed transitions, while for interstellar plasma's, forbidden lines are prominent. HII regions are a case in point. Explain this difference. In what interstellar environment do you expect that allowed recombination lines will far outshine forbidden transitions ?

13. Why does a molecule have so many more transitions than an atom ? Ignoring electronic excitation, in LTE at a fixed temperature, what does this mean for the internal energy of an H atom as compared to an H_2

molecule ? And, assuming equal mass, for the internal energy of an atomic hydrogen gas as compared to a molecular hydrogen gas ? How would this change at the low densities of the ISM ?

14. Compare the emission spectrum of CO gas at 10 K and 1000 K. Compare the emission spectrum of CO gas and C gas at 10 K. Explain the differences. For the same energy input, would CO gas be warmer, cooler, or at the same temperature as C gas ?

15. Radiative transfer of cooling lines has a large influence on the thermal structure of a cloud. Describe these effects qualitatively.

1.3 Chapter 3

1. Estimate the heating rate by stellar photons in an HII region, assuming a neutral hydrogen fraction of 10^{-3}. Adopt a total stellar ionizing photon luminosity of 5×10^{49} photons s^{-1}, a mean photon energy of 25 eV, a distance of 1 pc, and an average photo-ionization cross section $\alpha_H = 3 \times 10^{-19}$ cm^2.

2. Estimate the heating rate due to CI ionization (per H-atom) in an HI region due to the average interstellar radiation field for a neutral carbon fraction, f(CI). Adopt a mean CI photo-ionization cross section of 10^{-17} cm^2, a gas phase carbon abundance of 10^{-4}, a mean CI-ionizing photon intensity of 10^6 cm^{-2} s^{-1} sr^{-1}, and a mean photon energy of 12 eV. Compare your result to Eq. (3.8).

3. Estimate the photo-electric heating rate per H-atom due to the ionization of neutral PAHs in the average interstellar radiation field. Adopt an ionization potential of 6 eV, a mean photo-ionization cross section per C-atom of 7×10^{-18} cm^2, a fraction of the carbon locked up in PAHs of 0.05, an elemental carbon abundance of 3.5×10^{-4}, a mean ionizing photon intensity of 10^7 cm^{-2} s^{-1} sr^{-1}, and a mean photon energy of 10 eV. Compare your result to Eq. (3.17).

4. Estimate the cosmic ray heating rate. Adopt the interstellar proton cosmic ray flux after correction for Solar wind modulation (Fig. 1.11), an average cross section of 1 Å^2, 0.8 secondaries per primary ionization, and an average energy per ionization of 7 eV. Compare your result to Eq. (3.31).

5. Estimate the unattenuated X-ray heating rate. Adopt the photon flux and cross section for 125 Å($\simeq$ 0.1 keV; cf, Fig. 1.9 and 3.6), and a mean kinetic energy of the electron of 2 eV.

6. Estimate the H-column required for unit optical depth at 0.1 and 1 keV. Can you now understand the general behavior of the X-ray heating rate in Fig. 3.7 ?

7. Derive the expression for the Kolmogorov energy spectrum (Eq. 3.37).

8. Compare and contrast the important heating sources of ionized and neutral atomic gas.

1.4 Chapter 4

1. Using the potentials given (Eq. 4.11 and 4.13), derive the general expressions for the rate coefficients of neutral-neutral (Eq. 4.12) and ion-molecule (Eq. 4.14) reactions. Hint: Adopt an effective potential, $V_{eff}(r) = V(r) + L^2/2mr^2$, with $L = mvb$ the angular momentum in the collision (v and b are the velocity and impact parameter at large distances). The second term in this expression is the centrifugal barrier. Assume that a reaction will occur if this centrifugal barrier can be overcome. Thus, calculate the maximum impact parameter, which leads to orbiting of the colliding particles; e.g., at closest approach, the effective potential has to be zero. Then average this impact parameter over the Maxwellian velocity distribution.

2. Evaluate the energy absorbed/released in the reaction: CH + O $\longrightarrow$ CO + H at 0 K and atmospheric pressure using the heats of formation given in Table 4.5.

3. Chemical thermodynamics is an important tool for chemist. It will tell whether two species will react when brought together. If a reaction occurs, it will also provide the energy released and the equilibrium abundances of the species (reactants and products) involved. However, chemical thermodnamics will not provide reaction rates. Here, we will consider the reaction of H_2 with O_2 forming H_2O.

   (a) Write down this reaction.

   (b) Evaluate the energy absorbed/released at 0 K and atmospheric pressure using the heats of formation (change in enthalpies) given in Table 4.5 (Note the error in the first printing of the book. How did you guess that this was in error ?).

   (c) The equilibrium constant of a reaction, K_e, is given by $\Delta G = RT \ln K_e$ with ΔG the change in the Gibbs free energy and R the gas constant. The Gibbs free energy is given by $\Delta G = \Delta H - T\Delta S$ with ΔS the change in entrpy. Thus, a reaction will tend to proceed in the direction of decreased energy (negative ΔH) and maximum disorder (positive ΔS). At the low T of the ISM, we can ignore the entropy change. Calculate the equilibrium constant.

   (d) Do you think this reaction will occur in the ISM ? Explain your answer.

4. Cosmic ray ionization of molecular hydrogen leads to the formation of H_3^+. This species can transfer its "excess" proton to other species present

in a cloud. We will consider here: coronene and CO. If we assume that the degree of ionization is very low (eg., ignore recombination timescale), where would this extra proton eventually wind up.

5. Evaluate and plot the lifetime of the activated complex (Eq. (4.20)) as a function of energy (eg., n) for a fixed size of $s = 9$ and $s = 12$. Discuss your results.

6. Consider the molecule AB formed through the following reactions,

$$A + B \longrightarrow AB + h\nu \qquad k_1 \tag{1.3}$$

and

$$A + BC \longrightarrow AB + C \qquad k_2 \ , \tag{1.4}$$

and destroyed through the reactions

$$AB + D \longrightarrow A + BD \qquad k_3 \tag{1.5}$$

and

$$AB + h\nu \longrightarrow A + B \qquad k_4 \ . \tag{1.6}$$

Derive expressions for the steady state abundance of AB in terms of the abundances of the other species.

7. Consider a species physisorbed on a grain surface. Evaluate, as a function of binding energy (between 300 and 800 K), the evaporation timescale and the thermal hopping timescale at a temperature of 10 K and 30 K. Compare your results graphically with the rate of arrival of coreactants on a grain of 1000 Å for a gas phase density of coreactants of 1 cm^{-3}. CO is the main accreting species with a density of 10 cm^{-3}. If we assume that CO is chemically inert on a grain surface, evaluate (and compare) the rate at which newly accreted species are buried in the ice.

8. Assume that a newly accreted H atom can react with one CO or one O_3 molecule, evaluate the relative probability for reaction. Do the same for a newly accreted D atom. Compare these probabilities. What does this imply for deuterium fractionation on grain surfaces ?

9. Compare and contrast the various chemical gas phase reactions. Describe the "general" rules controlling gas phase routes in the ISM and their "rational".

10. Describe the various factors controlling surface reactions. Describe the "general" rules controlling grain surface routes in the ISM and their "rational".

11. Describe the pro's and con's of the various theoretical methods devised to describe grain surface chemistry.

1.5 Chapter 5

1. Extinction by dust in our galaxy is very patchy. Here, we will consider a cloud with a size of 5 pc, a hydrogen density of 50 H-atoms cm^{-3} and a dust-to-gas mass fraction of 10^{-2}. We will asssume spherical dust grains with a radius of 0.1 μm and a specific density of 3 g cm^{-3}. What is the visual extinction through this cloud if these grains absorb with unit efficiency ? If clouds are randomly distributed and the mean visual extinction is 1.8 mag kpc^{-1} in the plane of the Milky Way, on average, how many clouds are there per kpc ?

2. Because of radiation pressure, a dust grain at a distance r_o from a star with luminosity $L_\star$ will be accelerated to a terminal velocity,

$$v\,(term) \;=\; \left(\frac{3L_\star Q_{\mathrm{rp}}}{8cr_o a\rho_s}\right)^{1/2} \tag{1.7}$$

   with a the grain size, ρ_s the specific density of the grain material, and Q_{rp} the radiation pressure efficiency.

   (a) Derive this expression, starting from

$$F_{\mathrm{rp}} \;=\; C_{\mathrm{rp}}\,\frac{F}{c} \tag{1.8}$$

   with C_{rp} the radiation pressure efficiency. (Hint: $F \;=\; mvdv/dr$).

   (b) Calculate the terminal velocity for a grain radius of 0.1 μm, a specific density of 3 g cm^{-3}, a radiation pressure efficiency of 1, and a luminosity of 10^4 $\mathrm{L}_\odot$.

3. Derive equation (5.26) from equations (5.24) and (5.22).

4. The 2175 Å bump in the interstellar extinction curve is often represented by a Drude profile. In conductors, the valence and conduction bands overlap and electrons can be excited even by low energy photons. The optical response of the "free" electrons in conductors can be described by the Lorentz model without restoring forces and the dielectric constants are given by the Drude model (Eqn. (5.31) with $\omega_0 = 0$),

$$\epsilon \;=\; 1 \;-\; \frac{\omega_{\mathrm{p}}^2}{\omega^2 \;+\; i\gamma\omega} \tag{1.9}$$

   with real and imaginary parts,

$$\epsilon_1 \;=\; 1 \;-\; \frac{\omega_{\mathrm{p}}^2}{\omega^2 \;+\; \gamma^2} \tag{1.10}$$

$$\epsilon_2 \;=\; \frac{\omega_{\mathrm{p}}^2\gamma}{\omega\,(\omega^2 \;+\; \gamma^2)} \tag{1.11}$$

We will adopt here $\omega_{\rm p} = 8.7 \times 10^{15}$ s^{-1} and $\gamma = 1.9 \times 10^{15}$ s^{-1}. For spheres, this will result in a feature centered at 2175 Å with a width of 1 μm^{-1}.

(a) Calculate the optical constants between 1400-4000 Å and the extinction profile for spheres in the Rayleigh approximation (Eqn. (5.26). Check that peak and width correspond to those observed in the interstellar extinction curve.

(b) Calculate the extinction properties for small disks. Compare the peak and the profile in this case with those in the case of a sphere.

(c) Demonstrate that the shift in peak position is given by $\sqrt{L}$.

5. Derive equation (5.34) from equations (5.33) and (5.32).

6. Calculate the temperature of a silicate grain in the diffuse interstellar medium, adopting the Planck mean efficiencies given in equation (5.35), a UV absorption efficiency of unity, and an integrated interstellar photon radiation field, $4\pi\mathcal{N}_{IRSF} = 10^8$ photons cm^{-2} s^{-1} and a mean photon energy of 10 eV.

7. Consider a comet with a radius of 1 km and a mean density of 1 g cm^{-3} at a distance of 4 AU from the Sun.

   (a) Calculate the temperature, assuming that the comet can be represented by a black body.

   (b) Calculate the temperature of a 0.1 μm silicate dust grain ejected by this comet (use eqn. (5.35) in the IR and a UV/visual absorption efficiency of 1).

   (c) If the Deep Impact mission had catastrophically destroyed this comet into a big cloud (eg., all dust grains see the same Solar radiation field) of 0.1 μm fragments, calculate the total IR emission. Compare this to the IR emission of the comet itself.

8. Assuming a balance between the photo-electric effect and electron collisions, calculate the grain charge and potential in the IC63 PDR ($G_0 = 6 \times 10^2$, $n_e = 6$ cm^{-3} and $T = 200$ K). Adopt a work function of 5 eV.

9. Generally for PDRs, $G_0/n \sim 1$ and hence $\gamma \sim 10^5$. The resulting high grain potential reduces then the photoelectric effect substantially. We will examine the implications here. Start with equation (5.59) and assume, for simplicity, a constant UV dust absorption cross section, $\sigma_{\rm d}$, a constant yield, Y (adopt $Y = 0.1$), and approximate the FUV photon field by $4\pi\mathcal{N} = 1.5 \times 10^{-8}\,(\nu_H/\nu)^3\,G_0$ photons cm^{-2} s^{-1} Hz^{-1}. Balance this with collisional electron charging (Eqn. (5.51)) with a sticking coefficient, s_e, of unity and a reduced rate, $\tilde{J}$, given by $(1 + Z_d e^2/akT)$. Realize now that if $Z_d \gg 1$, the integration limit in equation (5.59) is linked to ionization potential and the grain charge by $Z_d e^2/a = h\nu_{Z_{\rm d}} - W$. Introducing the

following parameters, $x = \nu_{Z_d}/\nu_H$, $x_d = W/h\nu_H$, $x_k = kT/h\nu_H$, and $\gamma_1 = 2.9 \times 10^{-5}\,\gamma$ with $\gamma = G_0 T^{1/2}/n_e$, we can rewrite the ionization balance to

$$x^3 + (x_k - x_d + \gamma_1)\, x^2 - \gamma_1 = 0 \tag{1.12}$$

(a) Derive this equation.

(b) We will assume that $x_k \ll x_d$. When the photo-electric ejection rate is small, $\gamma_1 \ll x_d$ and we are in the limit of uncharged grains. Derive an expression for the grain charge in this limit (assume $x - x_d = \delta$ with δ small). Because of the various approximations, these results are slightly different from eqn. (5.81) in the book. Calculate the grain charge for a 1000 Å grain.

(c) Again, we will assume that $x_k \ll x_d$. When the photo-electric ejection rate is large, $\gamma_1 \gg x_d$ and the grains will be highly charged. Derive an expression for the grain charge in this limit (assume $1-x = \delta$ with δ small). Calculate the grain charge for a 1000 Å grain.

(d) The heating rate is given by

$$n\Gamma_d = n_d \sigma_d Y \int_{\nu_{Z_d}}^{\nu_H} 4\pi \mathcal{N}\,(h\nu - h\nu_{Z_d})\; d\nu \tag{1.13}$$

For the total dust cross section, $n_d\sigma_d$ per unit volume, adopt $5 \times 10^{-22}\delta_{uv} n$ cm $^{-1}$ with n the density of H nuclei and δ_{uv} the increased dust cross section compared to classical grains (responsible for the visual extinction; $\delta_{uv} = 1.8$). The heating rate can then be written as,

$$n\Gamma_d = 2.7 \times 10^{-26}\, \delta_{uv} n G_0 \left[\frac{(1-x)^2}{x}\right] \quad . \tag{1.14}$$

Derive this expression. Note that the heating decreases with increasing grain charge because fewer photons can further ionize a grain and because the energy per ionization is less. Derive limiting expressions for large and small γ_1.

(e) Calculate the heating rate as a function of density, using an electron abundance of 1.5×10^{-4}, $T = 300$ K, and $G_0 = 10^{-5}$. (Hint: solve the grain ionization equation for γ_1 as a function of x and derive for the adopted x the value of n). Compare your result with the results from Eqn. (3.16) and (3.17) in the book. Note the differences for large γ_1 (low density). This reflects the presence of a charge distribution which the formalism in the book takes into account.

The notation is slightly different from the book because it adheres to the formalism first developed by de Jong, T., 1977, A & A, 55, 137.

10. The grain size distribution.

(a) Adopt the MRN grain size distribution (Eqn. (5.97)), calculate the total surface area and total volume of interstellar dust grains.

(b) Calculate the fraction of the surface area in grains less than 200Å and the fraction of the total volume in grains larger than 200 Å.

(c) Suppose the grain size distribution extends into the molecular regime (e., down to 5 Å). Again, calculate the fraction of the surface area in grains less than 200Å.

11. Compare and contrast the processes that heat and cool interstellar dust to those of interstellar gas. Do you expect dust to be hotter or cooler than gas in HII regions ? And in neutral atomic regions ? And in molecular clouds ? Explain your answer.

12. Compare and contrast the processes that contribute to the charging of interstellar dust and the conditions when they dominate.

13. Describe the various methods to determine the mass of interstellar dust and their results.

14. Describe the various methods to determine the sizes of interstellar dust and their results.

15. Summarize the composition of interstellar dust and the observations supporting their identification.

1.6 Chapter 6

1. In this exercise, we will contrast the absorption and emission characteristics of a 50 C-atom PAH molecule with a spherical graphite dust particle with a radius of 100 Å (and a specific density of 2.2 g cm^{-3}).

   (a) Calculate the radiative equilibrium temperature of the graphite grain in the interstellar radiation field (cf., Eqn. (5.42)).

   (b) If we assume that both the PAH and the dust grain are at 20 K, calculate the energy content (in eV) of each, given a energy per mode of 0.05 cm^{-1}.

   (c) Calculate the UV absorption timescale for the PAH molecule (Eqn. (6.4)) and for the graphite grain (adopt the interstellar UV radiation field, (eg., $G_0 = 1$ or $4\pi\mathcal{N}_{\rm UV} = 10^8$ photons cm^{-2} s^{-1}) and a UV extinction efficiency of 1).

   (d) Assume that each absorbs a 10 eV photon. Calculate the temperature of each immediately after absorption. (Hint: For the PAH use Eq. (6.18). For the dust grain, assume a heat capacity given by, $C_{\rm V} = 3.84 \times 10^2\, VT^2$ erg K^{-1}, which results in a slightly higher temperature than Eqn. 6.18 would predict).

(e) The (energy) cooling rate ($k_{\rm E} \equiv dE/dt$) is given by

$$k_{\rm E}^{-1} = 4\pi \int_0^\infty \sigma(\nu) B(\nu, T)\, d\nu \qquad (1.15)$$

i. Calculate the cooling timescale for the dust grain, adopting the expression for the Planck mean efficiency for graphite grains (Eqn. (5.36)).

ii. Calculate the cooling timescale for the PAHs, assuming that their emission is dominated by one mode at 1600 cm^{-1} with an integrated strength of $\sigma = 4 \times 10^{-7}$ cm^{-2} Hz^{-1} $(\text{C-atom})^{-1}$.

iii. Derive expressions relating the temperature cooling timescale (dT/dt) to the energy cooling rate. (Hint: use Eqn. (6.18) for the PAH and the expression for the heat capacity for the grain given above). Evaluate these expressions immediately after UV photon absorption.

(f) Following Figure 6.5, sketch the time dependence of the temperature of the PAH and the graphite grain over an interval of a year. How will this figure change if G_0 increases to 10^5, appropriate for a PDR ? Explain your answer.

(g) When the emitters are not in radiative equilibrium, we can approximate the IR intensity by

$$I(\nu) = n_i \sigma_i B(\nu, T)\, \frac{k_{\rm UV}}{k_{\rm E}} \qquad (1.16)$$

evaluated directly after absorption. Calculate the IR spectrum assuming a density of PAH of $3 \times 10^{-7} n$ and a density of small graphite grains of $2 \times 10^{-9} n$. For the emission properties adopt the single mode at 1600 cm^{-1} for the PAH and a β-law (Eqn. (5.32)) for the dust ($\beta = 1.2$ is appropriate for amorphous carbon grains). In addition, assume the presence of 2000 Å dust grains in radiative equilibrium with the interstellar radiation field at 20 K and with an abundance of 4×10^{-13} per H nuclei (set $k_{\rm UV}$ equal to $k_{\rm E}$ for radiative equilibrium).

(h) Plot these spectra and compare them to the observed IR spectrum of the interstellar medium (Fig. 5.13). Realize that the actual spectrum of the small dust grains will be somewhat broadened to longer wavelengths. How will these spectra change if G_0 increases to 10^5 appropriate for PDRs ? Explain your answer.

2. The ionization balance for PAHs:

(a) Derive equation (6.58) for a PAH with two accessible ionization stages, neutral and singly ionized.

(b) As for dust grains, the ionized fractions of PAHs are given by equations (5.49) and (5.50). Consider coronene in the diffuse ISM. The various rates involved in the ionization balance are given in Table 6.2. Calculate the charge distribution and compare to Figure 6.7 (γ in Figure 6.7 is defined as $G_0 T^{1/2}/n_e$).

3. Unimolecular reactions involving PAHs:

   (a) Adopt the Arrhenius dissociation rate for the unimolecular reaction (Eqn. (6.73)) and calculate the H-loss rate from coronene assuming a critical energy of 3.3 eV and a pre-exponential factor of 3×10^{16} s^{-1} after absorption of a 10 eV photon.

   (b) With an IR cooling timescale of 1 s, what is the probability of dissociation ?

   (c) Recalculate the probability for dissociation if the molecule has lost 2 eV through IR radiation.

   (d) With the UV absorption rate given by equation (6.4) and an association rate of 2×10^{-8} cm^3 s^{-1}, calculate the fraction of circumcoronene molecules that will have lost an H-atom in the diffuse ISM ($G_0 = 1$, $n = 50$ cm^{-3}).

   (e) What will this fraction be in a PDR ($G_0 = 10^5$, $n = 10^5$ cm^{-3}) ?

4. Derive equation (6.86) from $f_{IR}/(1 - f_{IR}) = \tau_{FUV}(PAHs)/\tau_{FUV}(dust)$. With $f_{IR} = 0.13$, check that the abundance of 50 C-atom PAHs is 3×10^{-7} per H nuclei.

5. Describe the heating and cooling of interstellar PAHs and make a comparison with the heating and cooling of large interstellar dust grains. In this, focus on understanding figure 6.5.

6. Compare and contrast the processes that contribute to the charging of interstellar PAHs and contrast them to those involved in the ionization balance of interstellar dust.

7. Discuss the photochemistry of interstellar PAHs

8. Describe the infrared characteristics of interstellar PAHs and discuss how size and abundance of interstellar PAHs can be derived from the observations.

9. Compare and contrast the characteristics (temperature, spectra) of interstellar PAH, fullerenes, nano-diamonds, and nano-silicon.

1.7 Chapter 7

1. The ionization structure of HII regions containing only H:

(a) Calculate the stellar photon radiation field at a distance of 0.5 pc from an O4 star (Table 7.1). What is the timescale for ionization of a neutral H atom due to this radiation field if the average ionization cross section is equal to $5 \times 10^{-2}\alpha_0$ (with the threshold ionization cross section, α_0 equal to 6.3×10^{-18} cm^2) ?

(b) The recombination timescale for a proton is given by $(\beta_B n_e)^{-1}$ with $\beta_B = 2.6 \times 10^{-13}$ cm^3 s^{-1} the recombination rate coefficient to all levels with $n \geq 2$. Assume that essentially all H is ionized, compare these timescales and derive the neutral fraction at a density of 10^3 cm^{-3}.

(c) Following the same procedure, what is the neutral fraction at a distance of 1 pc from an O4 star ?

(d) Adopt an average neutral fraction of 10^{-3} in the nebula and calculate the optical depth for stellar photons at a distance of 0.5 pc and 1 pc, respectively.

(e) Derive equations (7.21) and (7.22) from equations (7.19) and (7.20).

(f) Plot the neutral fraction and the optical depth through an HII region with a density of 10^3 cm^{-3} ionized by an O4 star.

(g) Calculate the Strömgren radius of an HII region ionized by an O4 star with a density of 10^3 and 10^4 cm^{-3}, respectively. Check that the HII region with the lower density has a higher mass of gas. What is the origin of this apparent contradiction ?

2. The effect of dust on the ionization structure of HII regions:

(a) Substitute equation (7.19) into equation (7.45) and make the assumption $1 - x \ll 1$ and the substitution $\tau = \ln u$ to arrive at equation (7.46).

(b) Derive the solution, equation (7.47), by substituting $y = u \exp[\tau_d z]$ and using the standard integral

$$\int x^2 \exp[ax]\, dx = \frac{exp[ax]}{a} \left(x^2 - \frac{2x}{a} + \frac{2}{a^2} \right) \tag{1.17}$$

and the boundary conditions $tau(z = 0) = 0$.

(c) Get the correct expressions for equations (7.48) and (7.49) from the errata. Derive the right-hand-side of these equations from the left-hand-side and derive equation (7.50) from equations (7.48) and (7.49).

(d) Write down the expression for the size, z_0 of the HII region in the presence of dust. Plot the size of the HII region as a function of τ_d (Hint: This transcendental equation is readily solved by substituting $y_0 = \tau_d z_0$, realizing that $6/\tau_d^3 = 6z_0^3/y_0^3$, and solving for z_0 for given y_0. The τ_d corresponding to a resulting z_0 can then be found from y_0.)

3. Here, we will consider the ionization structure of trace species with Neon as an example. Neon has three relevant ionization stages for HII regions (eg., Ne^0 with an IP of 21.6 eV, Ne^+ with an ionization potential of 41 eV, and Ne^{2+} with an ionization potential 54 eV, the ionization potential of He^+): we will label these 0, 1, and 2. The relevant ionization cross sections averaged over a 50000 K black body are equal to $\alpha_0 = 8 \times 10^{-18}$ cm^2 and $\alpha_1 = 8 \times 10^{-18}$ cm^2. The radiative recombination rates are given by $\beta_1 = 2.2 \times 10^{-13}$ cm^3 s^{-1} and $\beta_2 = 2.2 \times 10^{-13}$ cm^3 s^{-1} at $T_e = 10^4$ K. For simplicity, we will adopt a black body radiation field and consider only ionization by the stellar radiation field.

   (a) The abundances of the three ionization stages –relative to the total Neon abundance – are given by

$$X_1 = \left(1 + \frac{\beta_1}{\alpha_0\, 4\pi\mathcal{N}_0} + \frac{\alpha_1\, 4\pi\mathcal{N}_1}{\beta_2}\right)^{-1} \tag{1.18}$$

$$X_0 = \frac{\beta_1}{\alpha_0\, 4\pi\mathcal{N}_0}\, X_1 \tag{1.19}$$

$$X_2 = \frac{\alpha_1\, 4\pi\mathcal{N}_1}{\beta_2}\, X_1 \tag{1.20}$$

   where z is $R/\mathcal{R}_s$ and $4\pi\mathcal{N}_i$ are the relvant stellar ionization photon fields. Derive these expressions from the ionization balance equations and the conservation equation.

   (b) Calculate the ionization parameter, U – as defined in equation (7.34) – for an O4 star and a density of 10^3 cm^{-3}.

   (c) The relevant ionizing radiation fields can be written in terms of the ionization parameter as,

$$4\pi\mathcal{N}_i = \frac{cUf_i}{z^2}\left(1 - z^3\right) \tag{1.21}$$

   The factors f_0 (0.32) and f_1 (0.021) are the fractions of the stellar ionizing photon radiation field that can ionize Ne^0 and Ne^+. The z^2 factor takes spherical dilution into account while the $1 - z^3$ factor accounts for attenuation. Derive this expression (hint: use equation (7.21)).

   (d) Plot the ionization structure of Neon as a function of z for this ionization parameter as well as for an ionization parameter corresponding to a density which is a factor 10^2 higher. Discuss these results by comparing and contrasting them with each other as well as with those for O and N in Figure 7.4.

4. Derive equation (7.58) from (7.57). Solve equation (7.58) and compare your results with figure 7.7 (Hint: solve for T_H as a function of T_e over the relevant range).

5. Consider an HII region heated by photo-ionization of H and cooled through emission by transitions of [OIII]. Solve the energy balance equations (7.59)-(7.61) and show that the electron temperature is approximately 7000 K under the assumptions used in these equations.

6. Solve the energy balance for the HII region in the previous excercise assuming an [OIII] abundance which is a factor of 3 higher. [Hint: for simplicity, treat each of the [OIII] finestructure levels as a two level system (cf., Eqn (2.30)). Relevant parameters are given in Table 2.6].

7. Derive Equations (763) and (7.64) from equation (7.62).

8. Derive Equation (7.71). Use Equation (7.68) to write an expression for the radio emission in the high and low optical depth limits in terms of the electron temperature, emission measure and frequency. Sketch the radio spectrum for an emission measure of 10^3, 10^6, and 10^9 cm^{-6} pc. Explain your result.

9. HII regions and the "energy balance" of the Milky Way

   (a) Adopt for the typical HII region in the Milky Way an average density of 30 cm^{-3} and an average ionizing photon energy of 20 eV, calculate the total cooling rate per atom.

   (b) Adopting the total mass in HII regions given in Table 1.1, calculate the total luminosity of ionzed gas in the Milky Way.

   (c) Adopting the physical characteristics of the WIM given in Table 1.1, calculate the total cooling rate per atom for this phase.

   (d) Adopting the total mass in the WIM given in Table 1.1, calculate the total cooling luminosity of this phase in the galaxy.

   (e) Comparing these values with those derived for the phases of the ISM (exercise 10 in chapter 2), explain why – on a galaxy-wide scale – ionized gas is so much more luminous than neutral gas.

   (f) Compare the derive total luminosity originating from ionized gas with the stellar radiative luminosities and the dust far-IR luminosity given in Table 1.3. What do you conclude ?

10. Describe qualitatively the ionization structure and energy balance of HII regions, focussing on the Strömgren sphere, the neutral fraction, the ionization front, and the effects of helium, trace species, and dust.

11. Describe the emission characteristics of HII regions.

12. Describe how the observed spectra of HII regions can be analyzed to determine the physical characteristics of the gas and ionizing star.

1.8 Chapter 8

1. The ionization balance:

    (a) Derive Equation (8.3) for the ionization balance of carbon in the diffuse interstellar medium, balancing photo-ionization with radiative electron recombination.

    (b) Derive expression (8.4) for the ionization balance in the presence of PAHs. For carbon, include photo-ionization and recombination with PAH anions. For PAHs, assume that radiative association of electrons with neutral PAHs is balanced by photo-ionization of PAH anions (eg., ignore the presence of PAH cations; cf., Fig. (6.7)).

    (c) Derive equantion (8.9) for the degree of ionization of hydrogen by assuming that cosmic ray ionization is balanced by proton-electron recombinations.

    (d) How is equation (8.9) modified in the presence of PAHs (eg., as for the C^+ ionization balance assume that cosmic ray ionization of H is balanced by H^+-PAH^- recombination; cf., exercise 1b).

2. The energy balance:

    (a) Derive equations (8.10), (8.11), (8.12) and (8.13) by balancing the appropriate heating and cooling processes.

    (b) The loci of thermal equilibrium for interstellar gas can be found directly from the cooling curve. At low densities, the ratio of the cooling rate per atom ($n\Lambda(T)$) to the thermal pressure (nT) is equal to $\Lambda(T)/T$ and is independent of density. This function is shown in Figure 1.2 for a low electron fraction (cf., Figure 2.10). Following Field, Goldsmith and Habing – the pioneers of interstellar thermal equilibrium studies – we will only consider heating by cosmic ray ionization,

    $$\Gamma_{\rm CR} = 3\times 10^{-27}\left(\frac{\zeta_{\rm CR}}{2\times 10^{-16}\ {\rm s}^{-1}}\right) \qquad {\rm erg\ s}^{-1}. \qquad (1.22)$$

    For a constant pressure $P/k = 3000$ cm^{-3} K, estimate the characteristics of the phases of the ISM adopting a primary cosmic ray ionization rate of 2×10^{-16}, 2×10^{-15}, and 2×10^{-14} s^{-1}. Explain your answer.

3. Derive the vertical density distribution (eqn. (8.23)) from the equation for hydrostatic equilibrium (eqn. (8.22)), assuming a isothermal layer.

4. The filling factor of the HIM plays a central role in the structure of the interstellar medium.

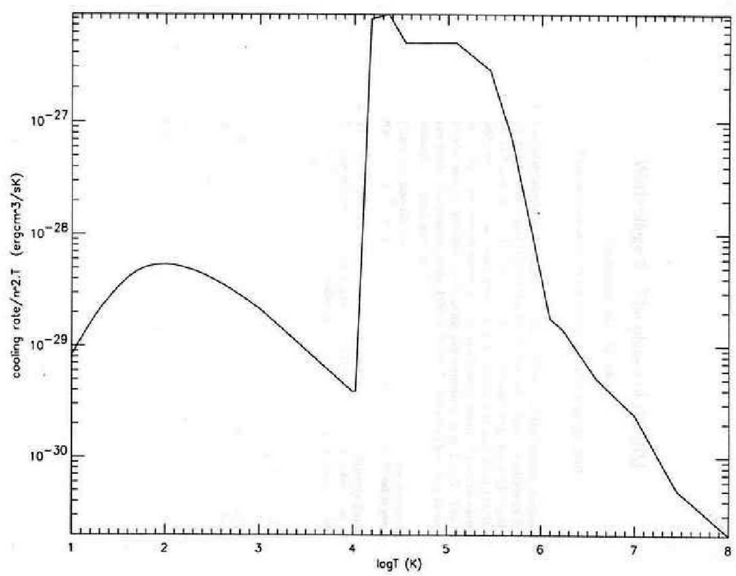

Figure 1.2: *The low density cooling rate for interstellar gas as a function of temperature is plotted in the form* Λ/T.

(a) Assume that the hot gas inside a SNR occupies an average volume, $V_{\rm snr}$, and survives for a time, $\tau_{\rm sn}$. In addition, assume that supernova explosions occur randomly in the galaxy at a rate of k_{sn} per unit volume and per unit time. Derive equation (8.33) for the filling factor of the hot gas in the galaxy. (hint: The rate of change of the probability that a point is inside a SNR, f is given by $df/dt = -f/\tau_{\rm sn} + (1-f)k_{\rm snr}V_{\rm snr}$).

(b) Basically this derivation assumes that SN do not explode within an existing cavity. Or to phrase it differently, the SN rate has to be corrected downwards for SN that do explode within existing cavities while the final volume and lifetime have to be corrected upwards for the rejuvenation associated with those SN that do explode within existing cavities. There is some discussion on this in Chapters 8.5.4 and 13.3. Adopt an effective supernova rate of $k_{sn} = 5 \times 10^{-5}$ yr^{-1} kpc^{-3} (an effective timescale for SN explosions of 8×10^{-3} yr^{-1} in the galaxy), which accounts for correlated SNe. The final volume and lifetime should be corrected by increasing the energy released by SNe in eqn. (8.29) and (8.30). Following the discussion in Chapter 13.3, this increase is only modest ($E_{\rm SN} \simeq 1.5 \times 10^{51}$ erg). These two parameters depend actually mainly on the ambient density. Adopting an ambient density of 0.5 and 3×10^{-3} cm^{-3}, calculate the filling factor of the HIM.

(c) We can also approach this problem from the opposite point of view where we use Poisson statistics to evaluate the probability that a SN explodes within a pre-existing cavity under the assumption that SNR do not interact. Derive this expression and calculate the filling factor (hint: consider a Poisson process with an average normalized SNR volume Q).

5. The photo-destruction of H_2 is controlled by the penetration of FUV photons into the cloud. Calculating the dissociating photon-flux at a given depth is of course the same problem as calculating the photon flux escaping from that depth; eg., the self-shielding factor (Eq. (8.40)) is analogous to the escape probability. Often the opacity is dominated by H_2 molecules located between the point under consideration and the surface. Here, we will look at this in some more detail. Consider a plane-parallel slab and an FUV flux incident perpendicular to its surface and one molecular line characterized by a peak frequency, ν_0, and a damping width, γ, which is the inverse of the lifetimes. The self-shielding factor is then

$$\beta_{ss}\left(N\left(H_2\right)\right) = \int_0^\infty H\left(a,v\right)\,\exp\left[-\tau_0 H\left(a,v\right)\right]\,dv \quad , \tag{1.23}$$

with $v = (\nu - \nu_0)/\Delta\nu_D$ the normalized frequency and $a = \gamma/\Delta\nu_D$ the normalized damping constant where $\Delta\nu_D$ is the Doppler width of the line. The optical depth at line center is given by $\tau_0\, a\,/\sqrt{\pi} = \left(\pi e^2/m_e c\right)\,\left(fg/\gamma\right) N\left(H_2\right)\, a/\sqrt{\pi}$ with f the oscillator strength and g the statistical weight. The line profile is described by the well-known, normalized Voigt function, $H\left(a,v\right)$, which can be approximated by a Doppler core $\exp\left[-v^2\right]$ and a Lorentzian wing $a\sqrt{\pi}\,v^{-2}$. The average oscillator strength is $f \simeq 10^{-2}$, the average Einstein $A \simeq 10^9$ s^{-1}, the peak wavelength is $\simeq 1000$ Å, and the statistical weight is 1/4 and 3/4 for para and ortho hydrogen.

(a) Calculate the H_2 column density for which optical depth effects start playing a role ($\tau_0\, a/\sqrt{\pi} > 1$). Now you should understand the significance of N_0 in Eq. (8.40).

(b) Evaluate the self-shielding factor for high optical depth and show that it is given by $\beta_{ss} = \left(\tau_0\right)^{-1/2}$.

Note that the somewhat steeper dependence on H_2 column density in Eq. (8.40) reflects the effect of line-overlap. Also, this discussion ignores the intermediate optical depth regime which gives rise to the logarithmic portion of the so-called curve-of-growth. This is discussed in a different context in more detail in D. Mihalas, 1978, Stellar Atmospheres, Freeman & Co.

6. Assuming that H_2 formation on grains is balanced by H_2 photodestruction, derive equation (8.45) for the abundance of H_2. Then, noting the error in

equation (8.47), derive the total column density at which half the gas is molecular.

7. Adopting a molecular hydrogen formation rate coefficient of $k_d = 3 \times 10^{-17}$ cm^{-3} s^{-1}, quantitatively evaluate the fractional abundance of molecular hydrogen in the diffuse interstellar medium as a function of column density and compare to the data in Figure 8.6 (use $N_H = 5.9 \times 10^{21}\, E_{B-V}$ cm^{-2}).

8. Molecular hydrogen formation in the early universe.

   (a) In the early universe ($z < 100$), H_2 is formed through the H^- channel (eqn. (8.51), (8.52)). At this point in time, there is a small amount of residual hydrogen ionization ($X(e) \simeq 3 \times 10^{-4}$) left after recombination. Because of the expansion, the radiation temperature is given by $T_R = T_o(1+z)$ with $T_o = 2.73$ and photo-ionization of H^- is unimportant. Adopting a temperature of 300 K, calculate the abundance of H^-.

   (b) Here we will adopt a Hubble constant of $H_o = 100h = 67$ km s^{-1} and a ratio of the density to the critical density of $\Omega_b = 4 \times 10^{-2}$ with the critical density given by $n_{cr} \simeq 10^{-5} h^2$ cm^{-3}. The density is then given by $n = \Omega_b n_{cr}\,(1+z)^3$. For a closure parameter of unity, the relationship between time and z is given by $dt/dz = -H_o^{-1}\,(1+z)^{-5/2}$. Estimate the molecular hydrogen abundance around $z = 100$.

9. Molecular hydrogen formation on grain surfaces.

   (a) Derive the equations describing the surface abundance of atomic hydrogen in physisorbed and chemisorbed sites (eqn. (8.58)-(8.60)).

   (b) Explain why the abundance of atomic hydrogen in chemisorbed sites is 1/2.

   (c) Derive the equations describing physisorbed hydrogen (eqn. (8.62) and (8.63)) and the H_2 formation efficiency (eqn. (8.64)). Make sure that you understand the origin of each term in the latter equation; eg., take the appropriate limits in the original equations and rederive this equation.

10. Derive the relationship between the observed line strength and the HI column density (equation (8.78)).

11. Using Figure 2.10 on page 59, estimate the cooling time scale at a temperature of 3×10^5 K (page 311). What is the cooling timescale at a temperature of 3×10^6 K ? This difference in the cooling timescale is very important in the dynamical evolution of supernova remnants (Chapter 12.3).

12. For a Hα intensity corresponding to 3 Rayleighs, calculate the emission measure of the Warm Ionized Medium. Adopting a scale length of 1 kpc, what is the root-mean-square density ?

13. Absorption lines

    (a) The equivalent with of the R(0) absorption line of C_2 at 8757.7 Å is measured to be 0.9 mÅ towards the star ζ Oph. With an oscillator strength of 1.7×10^{-3}, what is the C_2 column density in this state.

    (b) The equivalent width of the Q(10) line at 8780.1 Å towards this star is 0.65 mÅ. The oscillator strength is 8.5×10^{-4}. This state is 200 K above ground. Assuming thermodynamic equilibrium, calculate the temperature of the absorbing gas.

    (c) Explain why pure rotational radiative transitions are not expected to affect the level populations of this molecule under conditions appropriate for diffuse interstellar clouds.

    (d) The rotational level populations in the ground vibrational state can be affected by electronic fluorescence. Electronic excitation after absorption of a photon followed by radiative decay to the ground state may leave the species in a different rotational state than from which it started. With a typical photon excitation rate of $6 \times 10^{-9}\, G_0$ s^{-1}, a collisional cross section of 5×10^{-16} cm^2, and a kinetic temperature of 100 K typical for diffuse clouds, estimate the range of density and interstellar radiation field intensity for which the level populations will probe the physical conditions in diffuse clouds. Discuss your results.

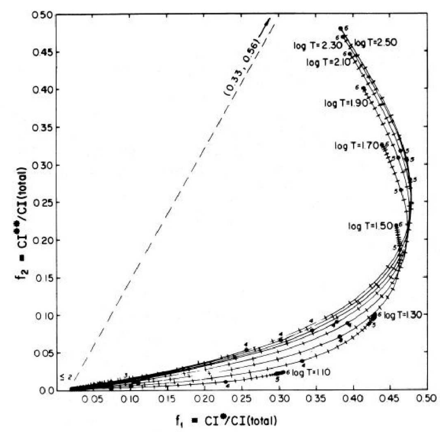

Figure 1.3: *The calculated ratio of the excited fine-structure levels,* $^3P_1$ *(C^*) and* $^3P_2$ *(C^{**}) relative to the total CI for various pressures and temperatures. The effects of UV pumping has been included as well in these calculations. The curves are labelled by log temperature and the labelled dots are density. Tickmarks indicate 0.1 in dex for density. Figure taken from Jenkins and Shaya (1979, ApJ, 231, 55).*

Table 1.1: Measured column densities of the finstructure levels of CI

Star	CI		CI ($^3P_1$)		CI ($^3P_2$)		T
	[cm^{-2}]	[cm^{-2}]	[cm^{-2}]	[cm^{-2}]	[cm^{-2}]	[cm^{-2}]	[K]
ζ Oph	15.25	15.35	14.90	15.10	14.27	14.33	75
o Per	15.45	15.75	14.58	14.78	14.18	14.38	48
ζ Per	15.44	15.52	14.11	14.36	14.04	14.14	57

[a] Taken from Jenkins and Shaya (1979, ApJ, 231, 55).

14. The population of fine structure levels is a sensitive measure of the density overthe density range their critical densities. Using the measured equivalent width of FUV absorption lines, the populations of the 3 CI ground state finestructure levels have been determined and these have been translated into pressure this way. This is more involved than the two level system discussed in chapter 2. Here, we will use the calculated ratios of the finestructure levels for different densities and pressures (Fig. 1.3) to take this last step. Table 1.1 gives the column densities associated with the CI fine structure levels towards three well-known stars. These are reported in terms of upper and lower limits.

    (a) Plot for each star the measured range in these ratios on figure 1.3 and determine the density range over the relevant temperature range shown. Estimate the pressure range allowed by the observations.

    (b) Using the temperature determined from the observed level populations of the lowest rotational levels of H_2 – which have very low critical densities and are thus expected to be in LTE –, what is the interstellar pressure along these sight lines ?

    (c) The populations can also be affected by FUV pumping. This has been included in figure 1.3 for the average interstellar radiation field. However, these diffuse clouds might be close to the star and hence the incident radiaion field may be much higher than the average interstellar radiation field. How would this affect the level populations ? And how does that influence the pressures that you determined ? Explain your answer.

15. Describe the processes that play a role in the ionization balance of the different phases of the interstellar medium.

16. Describe the processes that play a role in the energy balance of the different phases of the interstellar medium.

17. Describe the role of massive stars in the phase structure of the interstellar medium.

18. Discuss the formation and destruction of H_2 in the diffuse ISM.

19. Describe the chemistry of the diffuse ISM.

20. Discuss how the cosmic ray ionization rate can be determined from molecular observations.

21. Describe the emission characteristics of the different phases of the ISM and how the observations can be analyzed to derive the physical conditions in these phases.

1.9 Chapter 9

1. Derive equation (9.4) from equations (9.1)-(9.3) and the density-size relation of HII regions.

2. Write the ionization balance for carbon photo-ionization and C^+-e radiative recombination. Manipulate this equation to arrive at equation (9.6).

3. Compare the photo-ionization rate of magnesium with the cosmic ray ionization rate of H_2 and arrive at equation (9.7). Inserting a neutral Mg gas phase abundance of 3×10^{-6}, a primary cosmic ray ionization rate appropriate for dense clouds ($\zeta_{CR} = 3 \times 10^{-17}$, and the photo-ionization rate from Table 8.1, show that the depth in a molecular cloud where these two processes contribute equally to the ionization balance is $A_v \simeq 6$.

4. Balancing the photo-electric heating rate and the [OI] 63μm cooling rate, derive equation (9.8).

5. Balancing the photo-electric heating rate and the [CII] 158μm cooling rate, derive equation (9.9).

   (a) Starting from equation (9.15) arrive at equation (9.18).

   (b) Starting from equation (5.40) derive equation (9.19).

   (c) Explain (physically) why $\tau_{100\mu m}$ is independent of G_0.

6. Here, we will compare the intensities of the [CII] 158 μm and [SiII] 34.8 μm lines. We will consider the optical thin limit, assume that C^+ and Si^+ are the dominant ionization stages of carbon and silicon, and include only excitation by atomic H (and all hydrogen is atomic).

   (a) Give expressions for $n^2\Lambda$ as a function of temperature and density for [CII] and [SiII].

   (b) Give an expression for the [CII]/[SiII] line intensity ratio.

   (c) Plot the [CII]/[SiII] line intensity ratio for the density range of $10 < n < 10^7$ cm^{-3} at temperatures of 100, 300, and 1000 K.

   (d) Give a physical explanation for the general behavior of these curves, paying particular attention to the limits.

   (e) What density range is best probed by this ratio ? Compare this range to the critical densities of these transitions.

7. Explain the equation for the steady state timescale of H_2 (equation (9.24)).

8. Derive the relationship between the [CII] line flux and the total mass of the emitting gas (equation (9.33)).

9. The physical conditions in the NGC 2023 PDR

   (a) Estimate the intensity of the incident FUV field, G_0 from the observed infrared dust emission, using equation (9.29) and assuming a geometry factor of unity.

   (b) Estimate the temperature of the emitting gas from equation (9.31) (cf., Table 9.3), adopting a line width 5 km/s corresponding to a Doppler broadening parameter of 2.5 km/s.

   (c) Adopt this gas temperature and estimate from figure 9.2 (see errata) the gas density from the observed [CII]158μm/[OI] 63μm line ratio (cf., Table 9.3).

   (d) Estimate the photo-electric heating efficiency from the observed [OI] and [CII] line intensities and estimate the gas density from figure 3.4.

   (e) Use figure 9.9 to estimate the density and incident FUV field (cf., Table 9.3).

   (f) Calculate the total gas mass of the PDR associated with NGC 2023 (assume a [CII] line flux of 1×10^{-9} erg cm^{-2} s^{-1} and a distance of 450 pc).

   (g) Contrast your results with those for the Orion Bar (Table 9.1).

10. Discuss the interrelationship, similarities and differences of PDRs and HII regions.

11. Describe the chemistry of PDRs.

12. Describe the emission characteristics of PDRs and how the observations can be analyzed to derive the physical conditions.

1.10 Chapter 10

1. The ionization balance

   (a) Derive equation (10.1) for the degree of ionization by balancing cosmic ray ionization with the recombination of molecular cations with PAH anions.

   (b) Derive the equation for the degree of ionization in the absence of PAHs by balancing cosmic ray ionization with the recombination of metal cations with electrons.

(c) At a density of 10^5 cm^{-3}, calculate the expected degree of ionization for these two limiting cases. Adopt a primary cosmic ray ionization rate of 3×10^{-17} s^{-1}.

2. Derive equation (10.4) from equation (4.6) and (10.3).

3. Using figure 10.4 as a guide, derive equation (10.17). For an electron abundance of 10^{-7} and a CO abundance of 10^{-4}, calculate the deuterium fractionation of HCO^+ in a dark cloud. What is the expected fractionation in a hot core with a temperature of 200 K ?

4. Consider the chemistry involved in the cosmic ray ionization of H_2; viz.,

$$H_2 + CR \longrightarrow H_2^+ + e \tag{1.24}$$

$$H_2^+ + H_2 \longrightarrow H_3^+ + H \tag{1.25}$$

$$H_3^+ + CO \longrightarrow HCO^+ + H_2 \tag{1.26}$$

with the rates given in chapter 4. Adopt a CO abundance of 10^{-4} relative to H_2, calculate the steady state abundances of H_2^+ and H_3^+.

5. In dense cloud cores ($n \sim 10^6$ cm^{-3}) where all the CO has frozen out on grains, sequential reactions with HD, can drive deuterium fractionation all the way to D_3^+. Derive an equation for the D_3^+/H_3^+ ratio in this situation (cf., equation 10.19) and insert typical numerical values.

6. Inside a dense molecular cloud, atomic hydrogen is produced by cosmic ray ionization of H_2. Derive equation (10.24) by balancing H formation by cosmic rays with accretion of H on grains. What could be the cause of a higher atomic hydrogen abundance inside dense clouds ?

7. Accretion of ice mantles inside dense molecular clouds will increase the average grain size. All grains will acquire the same mantle thickness (cf., equation 10.25). Adopt the MRN size distribution for interstellar grains (equation 5.97) and calculate the increase in grain size if all the available gas phase oxygen (cf., Table 5.3) condenses out as H_2O.

8. Thermal spikes in a dust grain can lead to the ejection of a weakly-bound surface species. This process is discussed in section 6.4 in the context of the photochemistry of PAHs. The desorption probability, p_d, after a heating event is given by equation (6.82). For the IR cooling rate, k_{IR} adopt 1 s^{-1}. The unimolecular dissociation rate is given by equation (6.73) with equation (6.18) and (6.75). Calculate the critical grain size (e.g., for which $p_d = 1/2$) for an internal energy of 2 eV (cf., Figure 10.8).

9. Cosmic ray driven desoption of ice molecules

   (a) Using the expression for the heat capacity (equation (10.32), (10.33)), calculate the heat content of an ice grain as a function of temperature for a grain of 300Å and 1000Å radius.

(b) Evaluate the temperature of a 300 and a 1000 Å grain after passage of a 100 MeV/nucleon Fe cosmic ray ($\Delta E_{dep} = 5 \times 10^4 \left(a/1000\,\mathring{A}\right)$ eV).

(c) Evaluate the number ($N = \Delta E_{dep}/\Delta E_b$) of H_2O ($\Delta E_b = 0.5$ eV) or CO ($\Delta E_b = 0.05$ eV) molecules that evaporate.

(d) Evaluate the temperature of a 300 and 1000 Å ice grain when stored chemical energy is released by an 100 MeV/nucleon Fe cosmic ray. Adopt a radical concentration of 0.01 and 5eV per bond.

(e) Evaluate the number of H_2O or CO molecules that evaporate in this case.

10. CO line intensity

(a) For the CO $J = 1 - 0$ transition, derive equation (10.37) from equation (10.36).

(b) The brightness temperature, T_B, of a body which emits light with intensity $I(\nu)$ at frequency ν is defined as

$$I(\nu) = B(\nu, T_B) \tag{1.27}$$

Derive the relation between the brightness temperature and the observed integrated intensity of a line in the Rayleig limit

(c) Rewrite equation (10.36) in terms of the brightness temperature (equation (10.39)).

(d) Using the expression for the partition function of a linear molecule, derive the relation between the observed brightness temperature of the CO $J = 1 - 0$ transition and the total column density of CO.

11. Virial theorem and the molecular cloud mass

(a) Assume an isolated, homogenous spherical cloud with radius, R, mass, M and one dimensional velocity dispersion, σ. The internal kinetic and potential (gravitational) energy of this cloud are given by $E_k = 3/2\left(M\sigma^2\right)$ and $E_p = -3/5\left(GM^2/R\right)$ with G the gravitational constant. The Virial theorem states that $2E_k + E_p = 0$. The linewidth is then related to the mass and radius of the cloud - which apart from a small numerical factor is given by equation (10.46). Derive this relation, recalling that the linewidth and velocity dispersion are related by $\Delta v = \sqrt{8 \ln 2}\,\sigma$.

(b) Derive equation (10.47).

(c) Observationally, the one-dimensional velocity dispersion scales with the size of the cloud, $\sigma \simeq 0.55 R^{0.5}$ km/s (with R in pc) and the mass of the cloud (determined from CO isotopes) scales with the observed velocity dispersion, $\sigma \simeq 0.15 M^{1/4}$ km/s (with M in $M_\odot$).

i. Show that the observed CO luminosity of a cloud scales with the observed velocity dispersion.

ii. The average density ($\overline{\rho} = 3M/4\pi R^3$) is also observed to scale with the cloud size ($\overline{\rho} = 134 R^{-1}$ M$_\odot$ pc^{-3}). Show that this relation follows immediately from the above relations.

iii. The average density-size relationship implies that all molecular clouds have the same column density. Calculate the visual extinction corresponding to this column (cf., equation (5.96)). Compare this estimate to the depth to which photons contribute appreciably to the ionization of molecular clouds (exercise 3). What conclusion do you draw ?

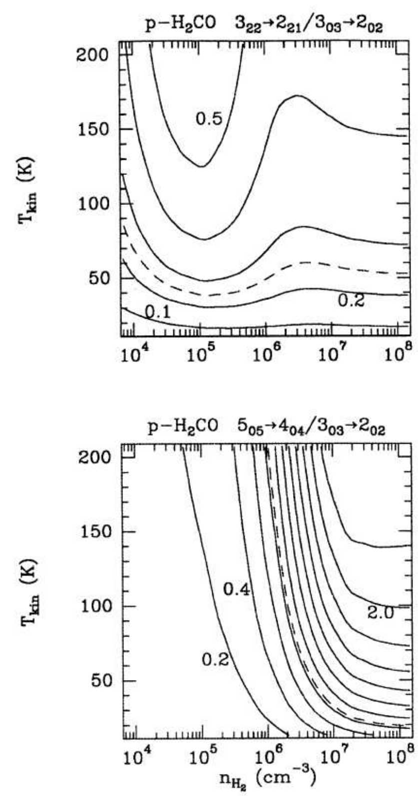

Figure 1.4: *Calculated ratios of para-H_2CO lines (taken from van Dishoeck et al., 1995, ApJ, 447, 760).*

12. Estimate the density and kinetic temperature from formaldehyde observations of the class 0 protostar, IRAS 16293-2422, using figure 1.4. The observed line intensities of para formaldehyde lines are 3.35 ($3_{22} - 2_{21}$),

Table 1.2: Characteristics of the ice bands observed towards NGC 7538 IRS 9[a]

Species	τ	λ [μm]	$\Delta\nu$ [cm^{-1}]
H_2O	3.0	3.1	440
CO	4.67	2.6	4.8
CO_2	15.2	0.8	21
CH_3OH	3.54	0.07	29
H_2CO	5.85	0.06	30
CH_4	7.6	0.09	11
$NH_3$9.0	0.2	68	

[a]Taken from Gibb et al. (2004, ApJS, 151, 35).

13.2 ($3_{03} - 2_{02}$), and 13.5 ($5_{05} - 4_{04}$) K km/s. If the line intensities are uncertain by 20% what is then the range in densities and temperatures ?

13. Determine the column densities of ice components observed towards NGC 7538 IRS 9. The ice band characteristics are given in Table 1.2. Translate this into abundances using the observed 10μm silicate optical depth ($\tau = 2.2$) and typical interstellar silicate properties (section 5.5.1). For comparison, the column density of gas phase CO towards this source is 1.4×10^{19} cm^{-2}.

14. Assume that inside dense cloud cores, the gas phase abundance of CO is set by the balance of accretion of CO molecules on grains and cosmic ray driven evaporation. What is the abundance of CO as a function of density if the ejection rate is $\simeq 10^{-17}$ CO molecules s^{-1} (largely driven by 100 MeV/nucleon Fe CR hits of small ice grains). Internal stored energy could raise this rate to $\simeq 4 \times 10^{-17}$ CO molecules s^{-1}. What is the abundance of gaseous CO in this case ?

15. Discuss the interrelationship, similarities and differences of diffuse and dark clouds.

16. Describe the flow of ionization in molecular clouds and its role in driving gas phase chemistry.

17. Link the observed molecular composition of interstellar clouds (gas and grains) back to the processes driving the chemistry.

18. Discuss the interaction between dust and gas in molecular clouds.

19. Describe the emission characteristics of molecular clouds and how the observations can be analyzed to derive the physical conditions.

1.11 Chapter 11

1. Manipulate equations (11.1), (11.2), and (11.6) to arrive at equation (11.13) and (11.14). Use these expressions together with equation (11.12) to arrive at equation (11.15) and (11.16). Examine the high shock velocity limit. What do you conclude about the pre- and postshock density and velocity contrast ? And the pressure and temperature ?

2. In the case of magnetic cushioning, derive the temperature corresponding to maximum compression (equation (11.31)).

3. Compare and contrast interstellar J and C shocks.

4. Discuss shock spectra and their diagnostic value.

1.12 Chapter 12

1. Derive equation (12.6) from the momentum and continuity equations. Evaluate the two critical shock velocities and examine the characteristics of those solutions.

2. During the initial phase of rapid ionization, derive an expression for the time dependent evolution of the ionized volume (equation (12.15)), starting from equation (12.12).

3. During the pressure-driven-expansion phase of the evolution of HII regions, derive an expression for the time dependent size of the ionized volume (equation (12.20)), starting from the momentum equation (equation (12.16)).

4. Consider the ionization of a neutral globule. Starting from equation (12.34), derive equations (12.39) and (12.40).

5. The book cover shows an IR image of the cometary globule, IC 1396A, and figure 1.7 shows an infrared view of the "pillars of creation" in the Eagle nebula. Here, we will compare the characteristics of these globules with the theoretical discussion in section 12.2.4.

   (a) The globule in IC 1396A is located at a projected distance of 3.8 pc from the O6.5 ionizing star, HD 206267. CO observations estimate the mass of this globule at $\simeq 200\ \mathrm{M}_\odot$, while the density is approximately $2 \times 10^4\ \mathrm{cm}^{-3}$. The size of the globule is 0.5 pc. The average density of the ionized gas is $\simeq 600\ \mathrm{cm}^{-3}$. Estimate the ionizing photon flux, $\mathcal{N}_\star$, at the base of the flow required to keep the flow ionized.

   (b) Pillar 1 in the Eagle nebula is located at a projected distance of 2 pc from the ionizing star cluster which contains several O5 stars with an estimated ionizing luminosity of 2×10^{50} photons s^{-1}. CO observations estimate the mass of this globule at $\simeq 9$ $M_\odot$, while the density is approximately 10^5 cm^{-3}. The 'radius' of the pillar is 0.1 pc. The average density of the ionized gas is $\simeq 500$ cm^{-3}. Estimate the ionizing photon flux, $\mathcal{N}_\star$, at the base of the flow required to keep the flow ionized.

(c) Compare these photon fluxes with those expected from the ionizing stars. What do you conclude ?

(d) Evaluate the mass loss rate from these structures and their expected lifetimes.

(e) The ionizing star of IC 1396A is a member of the cluster Trumpler 17 at the nucleus of the Cep OB2 association with an estimated age of $\simeq 4 \times 10^6$ years. The ionizing star cluster of the Eagle nebula is at the core of the Ser OB1 association and the estimated age is 2 Myr. What could cause this discrepancy between the stellar age and expected lifetime of the globule ? (hint: Examine the images in detail. Also consider the evolution of the region).

6. Derive equations (12.49) and (12.52).

7. Derive the density distribution in a plane parallel blister HII region (equation 12.62).

8. The Sedov Taylor expansion phase of supernova remnants.

   (a) For the Sedov-Taylor phase of a supernova blast wave expanding into an intercloud medium ($n = 0.5$ cm^{-3}) at 1000 km/s, evaluate the cooling timescale and compare this to a relevant dynamical timescale.

   (b) During the Sedov-Taylor expansion phase, the energy is conserved. Because of self-similarity, the characteristics of the supernova remnant depend on a combination of only three quantities: the explosion energy, E_{sn}, the density of the surrounding medium, ρ_0, and the time, t. Simple dimensional analysis yields then immediately that $R_s = (\xi_0 E_{sn} t^2/\rho_0)^{1/5}$ with ξ_0 a constant. Derive this equation. (Hint: write $R_s \sim E_{sn}^a \rho_0^b t^c$ and compare dimensions on the left- and right-hand-side.)

   (c) We can simplify the discussion in section 12.3.2 somewhat by assuming (incorrectly) that the supernova remnant is homogeneous. The total energy is then given by $E_{sn} = M\,(u_T + u_k)$ with M the total mass and u_T and u_k the internal and kinetic energy of the gas per unit mass. These we will set equal to the values just behind the shock front, $3/2\,P_1/\rho_1$ and $1/2\,v_1^2$. Then using the strong shock conditions (equations (11.18) and (11.19)) and recalling that the expansion velocity is equal to dR_s/dt, we arrive at equation (12.79) with $\xi_0 = 60/4\pi$. Derive this equation and the value of ξ_0.

(d) Figure 1.4 shows optical emission from the Cygnus loop, the prototypical middle-aged supernova remnant. The whole remnant is some 10 pc in size (depending on the somewhat uncertain distance). The observed X-ray luminosity of this supernova is $L_x \sim 10^{36}$ erg s^{-1}and the temperature of the gas is $T_x \simeq 3 \times 10^6$ K. Ignoring the density structure of the remnant, derive an expression for the luminosity of the supernova remnant in terms of the cooling rate, Λ, density of the surrounding medium, n_0, and the size, R_s. Use this expression to determine the density of the surrounding medium and the mass swept up by the supernova remnant.

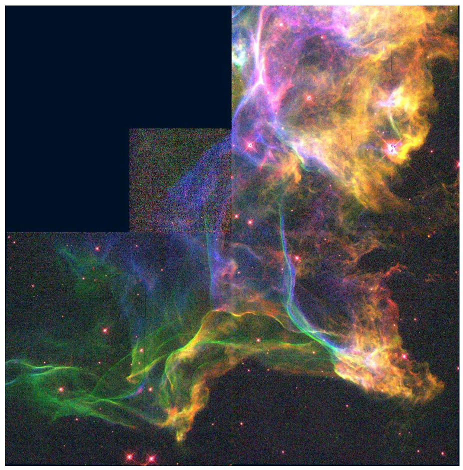

Figure 1.5: *False color image of the optical emission from the Cygnus loop. The supernova remnant expands from left to right. Blue indicates emission from [OIII], red is emission from [SII], and green is emission from HI.*

(e) Hα and [OIII] imaging of filaments in the northeast of the Cygnus loop have revealed that their characteristics vary systematically. Specifically, they show a transition from Balmer-dominated to [OIII]-dominated (Figure 1.5). What could be causing these variations ? What does this tell us about the shock velocity and the preshock density ? (Hint: Reread section 11.2.3).

9. During the radiative phase, the expansion of supernova remnants is controlled by momentum conservation (equation (12.83)). If we can ignore the external pressure, then the flow is self-similar again. Assuming that the size of the remnant scales with t^η with η a constant, derive the value of this constant.

10. During the evaporative phase of the expansion of supernova remnants, the expansion is controlled by the mass equation (equation (12.107)) and

energy conservation. Again, this flow is self-similar. Assume that the size of the remnant scales with t^η with η a constant and derive the value of this constant. (Hint: note that $T \sim v_s^2$.).

11. Show that for an evaporative SNR, the expansion law (equation (12.109)) can be written in the standard form of a Sedov-Taylor blast wave (equation (12.116)) but with a time-dependent density (equation (12.136)).

12. During the adiabatic phase of a hot wind bubble, the expansion is governed by the energy and momentum equations (equations (12.124) and (12.125)). Assuming that the size of the remnant scales with t^η with η a constant, show that the self-similar exponent describing the flow is $\eta = 3/5$. Explain why this expression is very similar to that describing the adiabatic phase of a SNR (equation (12.79)).

13. After reading the section on the structure of the dense shell (section 12.5.3) and recalling the discussion on radio emission from ionized gas (section 7.4.3), derive the limb brightening intensity profile of an ionized wind bubble.

14. Discuss the different phases in the expansion of HII regions and their characteristics.

15. Discuss the effects of inhomogeneities on the evolution of HII regions.

16. Discuss the different phases in the expansion of supernova remnants and their characteristics.

17. Compare and contrast the evolutionary characteristics of supernova remnants in a homogeneous ISM with a two-phase and three-phase ISM.

18. Discuss the characteristics of wind bubbles.

1.13 Chapter 13

1. Examine figure 13.2 and demonstrate that the increase in velocity for large grains is consistent with betatron acceleration.

2. Derive an expression for the collisional stopping length of grains moving at velocity v relative to the gas (ignore Coulomb focussing). Evaluate the stopping length for the grains and the physical conditions in the 100 km/s shock shown in figure 13.2. Check your answer against the results shown (Recall that $N_H = n_0 v_s t$). Using the charging discussion in section 5.2.3, check that Coulomb interaction is only a small correction to this result.

3. Explain why grains embedded in a hot gas decrease in size at a rate independent of size.

4. Estimate the sputtering yield for a carbon grain in a 10^6 K gas. How long would a 100 Å grain survive at 3 kpc in the lower halo of the galaxy ? How does this compare to a typical dynamical timescale ? Use the characteristics described in table 1.1.

5. Fraction of an element locked up in dust

   (a) Derive the expression for the rate of change in the fraction of an element locked up in dust (equation (13.12)). Develop the steady state solution to this expression.

   (b) Consider a two-phase medium where destruction occurs in the warm medium at a rate, k_{des}, while accretion accurs in the diffuse cloud medium at a rate, k_{acc}. Include the effects of mixing. Derive the expressions describing the fraction of an element locked up in dust in the diffuse cloud medium and in the intercloud medium (equations (13.14) and (13.15)).

6. Derive an expression for the fraction of silicates in the interstellar medium with a crystalline structure. Consider that a fraction, δ_c, is injected as crystalline silicates by stars while the remainder is in amorphous form. Assume further that crystalline and amorphous silicates are destroyed by interstellar shocks at the same rate. In addition, include the effects of cosmic ray ion bombardment which amorphize crystalline silicates at a rate k_{am}. Evaluate the fraction of silicates in the interstellar medium with a crystalline structure if $\delta_o = 0.15$, $k_{am} = (70)^{-1}$ Myr^{-1}. Use typical values for the other rates as given in section 13.5. Do you expect a difference in the crystalline fraction between the diffuse cloud phase and the warm intercloud phase ?

7. Discuss the lifecycle of interstellar dust and the processes that play a role in this cycle.

8. Compare and contrast the destruction of dust in adiabatic and radiative shocks.